International Journal of GEOMATE, Dec., 2024 Vol.27, Issue 124, pp.32-39
ISSN: 2186-2982 (P), 2186-2990 (O), Japan, DOI: https://doi.org/10.21660/2024.124.4606
Geotechnique, Construction Materials and Environment

EFFECT OF PVA SHORT FIBERS AND GEOGRID ON THE FLEXURAL STRENGTH OF CEMENT-MIXED SANDY SOIL

*Hekmatullah Fahimi[1], Taro Uchimura[2], Tufail Ahmad[3]

[1,2,3] Department of Civil & Environmental Engineering, Saitama University, Japan

*Corresponding Author, Received: 26 June 2024, Revised: 21 Oct. 2024, Accepted: 25 Oct. 2024

ABSTRACT: Cement-mixed soil has been widely used in road and railway construction. Mixing cement with soil increases its bearing capacity, stiffness, and shear strength while reducing the compressibility and volume changes of the soil. However, using only cement can lead to sudden and brittle failure due to the low tensile and flexural strengths of cement-mixed soils. In this study, the flexural strength and deflection behavior of cement-mixed sand, reinforced with geogrids (single and dual layers) and short fibers (0.5% and 1%), were investigated. Two types of biaxial geogrids were employed, along with polyvinyl alcohol (PVA) fibers measuring 12 mm in length and 0.1 mm in diameter. Standard silica sand and 6% ordinary Portland cement (OPC) Type I served as the sand and binding materials, respectively. Fifteen beam specimens, each measuring 15×15×53 cm, were prepared and cured for 28 days before testing. The experimental findings revealed that both the fiber content and the addition of biaxial geogrids improved the flexural behaviour of the cement-mixed sand. Specifically, incorporating fibers (0.5% and 1%) and dual-layer geogrids increased the first peak (f1) strength by 1.25 times and the peak strength by 2.53 times. Additionally, this reinforcement strategy enhanced crack patterns and distributed flexural loads across different parts of the beam specimens, resulting in multiple crack failure modes. Overall, the combined use of geogrids and fibers effectively reinforced the cement-mixed soil, producing a stress-deflection curve similar to that of steel bar-reinforced concrete, an improved failure mode, and the highest flexural strength.

Keywords: *Flexural strength, Cement-mixed sand, Biaxial geogrids, Polyvinyl alcohol fibers, Stress-deflection curve.*

1. INTRODUCTION

Cement-mixed soil has been used in road and railway construction. Cement-mixed sand, also called cement-stabilized sand, contains some low amounts of cement (usually less than 10%), sand, optimum water, and air. The cement material is mixed with sand to increase the bearing capacity, stiffness, and shear strength of the material. However, its low tensile and flexural strengths may cause sudden and brittle failure [1]. Moreover, owing to its low confining pressure and excessive traffic loads, this brittle behavior is more pronounced when cement-mixed soil is used at shallow depths, such as the subgrade, subbase, and base course layers. Ductility and toughness are necessary for pavement materials to avoid sudden failure and brittle behaviour after reaching their maximum stresses due to excessive traffic loads [2,3]. In current cement-mixed soil applications, synthetic and natural fibre materials are used to reinforce the cement-mixed soil and decrease its brittleness [4, 5, 6]. For example, Shen et al. used polyester fibres to investigate the flexural strength characteristics of cement and lime-stabilized clay [7]. Ateş. studied the mechanical properties of sandy soils reinforced with randomly distributed glass fibres [8], and their research results revealed that the addition of discrete randomly oriented fibres improved the load-deflection response that typically occurs in road pavement structures [3]. Sukontasukkul & Jamsawang used steel and polypropylene fibres to improve the flexural performance of deep soil cement columns [1]. However, the homogeneity and uniformity of mixing fibres, cement, and sand is not easy to maintain in practice. The nonuniformity of fibre reinforcement significantly reduces the fibre-reinforced soil strength [9]. Geogrids are also widely used as reinforcement materials in soil and concrete applications. Research has shown that geogrid reinforcement can increase the flexural strength and toughness of cement-treated sand; thus, it is more effective as a subbase layer in pavement construction [10]. Previous studies have focused on using fibres or geogrids separately. However, to decrease the non-homogeneity and nonuniformity effect of fibres, increase the flexural strength, and avoid brittle failure of the cement-mixed base and subbase coarse, the inclusion of both fibres and geogrids together is a more advantageous option. The geogrid can reinforce the cement mixed with soil against flexural stress. Therefore, if non-homogeneity occurs due to soil–fibre mixing, the geogrid will reinforce it. In this study, the flexural behaviour of cement-mixed sandy soil

reinforced with short fibres and geogrids is investigated. The parameters such as the stress–deflection curve, first peak flexural strength, peak flexural strength, and crack pattern were examined to evaluate the flexural performance of the cement-mixed soil. The experiments were performed using three-point bending testing of the cement-mixed soil.

2. RESEARCH SIGNIFICANCE

The application of cement-mixed soil at shallower depths, such as base coarse and subbase coarse depths, may cause sudden and brittle failure due to the low tensile and flexural strengths of cement-mixed soil. This study focuses on the flexural performance of cement-mixed soil reinforced with fibres and geogrids. The aim of this study is to address proper reinforcement that increases the flexural strength of cement-mixed soil and decreases its brittleness.

3. MATERIALS AND METHODS

3.1 Materials

3.1.1 Silica Sand

The sand utilized in this study was Nikko standard silica sand, which is a commonly employed material in laboratory research and readily available commercially in Japan. Since the naturally available sand used as treated sand material for road construction contains different sizes of particles [4, 11, 12], a blend of different grades of silica sand was prepared for use in the experimental study. After the silica mix preparation for the drying process, the sample was put in an oven for 24 hours at 105±5 C° temperature. The sieve analysis test was conducted to determine the particle size distribution curve. Fig 1 shows the particle size distribution curve of the silica mixture obtained from the sieve analysis results. Parameters such as coefficient of uniformity, coefficient of curvature and diameters corresponding to 10, 30, and 60% finer were determined from the particle size distribution curve given in Table 1. According to the Unified Classification System (UCS), the sand mixture was classified as poorly graded. The fibre used in this study was Polyvinyl Alcohol (PVA) fibre (Fig 2). PVA fibre is a synthetic fibre that was recently used in fibre-reinforced concrete [10]. The Table 4 shows the physical properties of the PVA fibre.

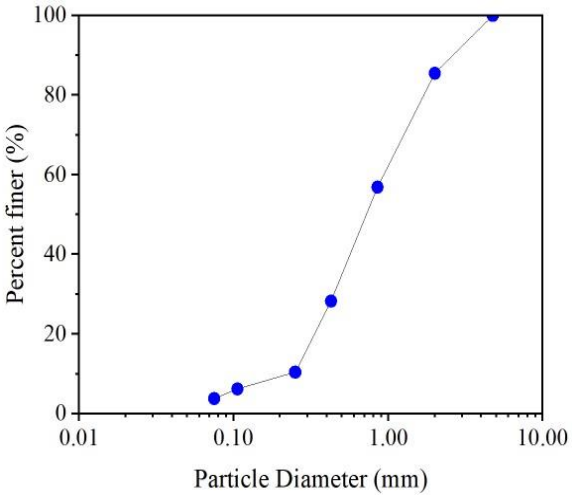

Fig 1.Particle size distribution curve of the silica sand

Table 1. Physical properties of the silica sand

Physical property	Value
Soil particle density, ρ_s (g/cm^3)	2.68
Gravel fraction 2.0~75 mm (%)	13.00
Coarse sand fraction 0.425~2.0 mm (%)	57.23
Fine sand fraction 0.075~0.425 mm (%)	24.46
Silt fraction 0.005~0.075 mm (%)	3.80
Uniformity coefficient, C_u	3.91
Curvature coefficient, C_c	0.91


Fig 2. Polyvinyl alcohol (PVA) short fibre

3.1.2 Geogrid

Two types of geogrid material were used: type-1 geogrids with the commercial name “SS2” (Fig 3a) and type-2 geogrids with the commercial name “KJV-W60” (Fig 3b). These geogrids, which had different aperture dimensions and tensile strengths, were used to reinforce the cement-mixed sand. Table 2 lists the properties of the type-1 geogrid, and Table 1 lists the properties of the type-2 geogrid.

3.2 Specimen Preparation

To prepare a cement-mixed-fibre-geogrid-sand (CMFGS) specimen, dry silica sand was mixed with the cement by hand for 5 minutes and then with the fibres for an additional 5 minutes [1,11]. Next, an optimum water content of 10.1% was obtained from the modified Proctor test and was added to the mixture. To ensure that the mixture was uniform and homogeneous, it was mixed for an additional 5 minutes. After lubricating the mould with a releasing agent, enough mass for a 2.5 cm portion was weighed and transferred to a mould with dimensions of 150 mm wide, 150 mm high, and 530 mm length. After putting the geogrid layer in its position, the remaining amount of the first one-third of the mix was transferred into the mould.

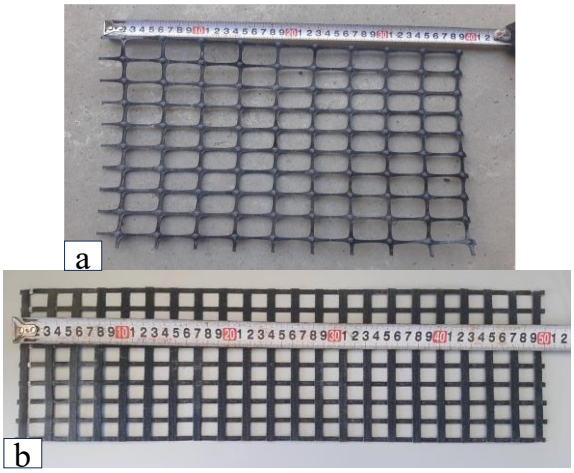

Fig 3.Types of geogrids: (a) type-1; type-2 (b)

Table 2. Properties of the type-1 biaxial geogrid

Item No	Property Name	Values	
1	Polymer	Polyester	
2	Typical unit weight, g/m^2	340	
3	Aperture Dimensions (Longitudinal/Transverse), mm/mm	40/28	
4	Junction Thickness, mm	3.90	
5	Junction efficiency, %	100~10	
6	Direction	Machine Direction	Cross-Machine Direction
7	Actual strength (kN/m)	22.30	37.90
8	Quality control strength (kN/m)	19	32
9	Design strength (kN/m)	17	30

It was followed by compaction with a wooden hammer and compression machine until the required dry density (1.92 g/cm^3) was reached [11]. Afterwards, the second one-third of the mix was weighted and transferred to the mould. After compaction, the remaining layer of the specimen was made in the same manner as the fibre cement-mixed sand specimen explained earlier. The top surfaces of the beam specimens were finished to obtain a flat surface. Table 5 provides the details of the prepared specimens and their reinforcement details. All 15 beam specimens were made in the same manner and wrapped in a special curing sheet [13] for curing. The prepared specimens were cured for 28 days before testing.

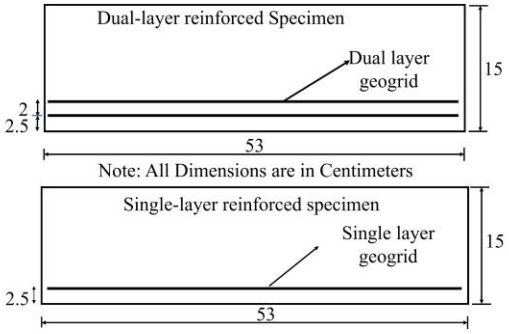

Fig 4. Geogrid reinforcement position in the beam

Table 3. Properties of the type-2 biaxial geogrid

Item No	Property Name	Value
1	Typical Unit Weight, g/m^2	600
2	Ultimate Tensile strength, kN/m	81
3	Design strength, kN/m	69
4	Stiffness at 1% strain, kN/m	1050
5	Aperture Dimensions, mm	23*15

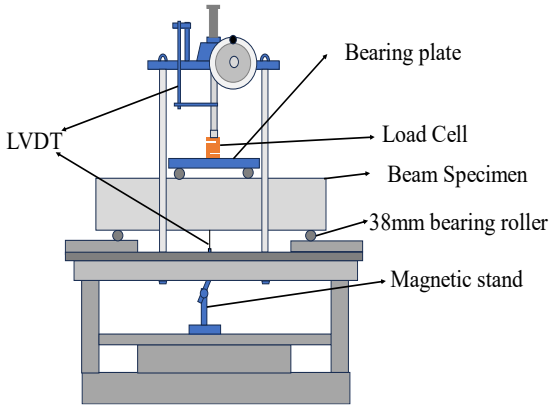

Fig 5. Setup for the bending flexural test

3.3 Test Procedure

After 28 days of curing [1, 11], the specimens were removed from the curing tank, and the special curing sheets were removed. To avoid surface drying, which could cause a decline in flexural strength, the specimens were prepared for testing immediately after curing. The specimens reinforced with geogrids were tested in the casting direction. Therefore, all specimens were tested in the same casting direction. The top of the specimen was ground to provide full contact between its top surface and the load-applying devices. All specimens were tested according to ASTM C1609/ 1609 M [14]. The test setup and equipment for the bending flexural test were set up as Fig 5. The specimens were placed on the roller supports, and two more rollers were attached from the top of the beam to apply two-point loads. A 20 kN load cell was employed to measure the applied load. The load cell was calibrated with a calibration machine before being attached to the testing machine. A dial gauge-type displacement transducer was used to monitor the beam deflection at the mid-span of the beam during the test. The displacement transducer was attached to the bottom of the beam at the midspan by a magnetic stand, as shown in Fig 5. The correlations among the waveform, load cell and displacement transducer were determined. The deflection rate was controlled at a deflection rate of 0.05–0.3 mm/min. The test was finished when the specimen failed.

4. DISCUSSION AND RESULTS

4.1 Characteristics of The Flexural Stress–Deflection Curves of The Fibre–Cement–Sand

Fig 6 shows the flexural stress–deflection curves of both fibre-reinforced and unreinforced cement-mixed sand. The shape of the deflection curves shows that adding PVA fibres improved the flexural characteristics of the cement-mixed sand. For the unreinforced specimens, the flexural stress increased in proportion to the deflection until the first crack occurred and its first peak strength (f1) was reached. Then, the strength suddenly decreased to zero [4, 15]. This finding indicated that the unreinforced specimens of cement-mixed soil showed brittle behaviour. For the cement-mixed specimens reinforced with only short

Table 4. Physical properties of polyvinyl alcohol (PVA) fibres

Materials	Specific gravity (g/cm^3)	Diameter (mm)	Length (mm)	Tensile strength (N/mm^2)	Young's Modulus (GPa)	Melting point (C^o)
PVA fibre	1.3	0.1	12	1200	28	225

Table 5: Specimen reinforcement details

Beam ID	Description Of specimen	Cement (%)	Fibre Content %	Geogrid Layer	Geogrid's type
CMS-0	Cement-mixed sand	6%	-	-	
CFS-1	Cement Fibre sand	6%	0.5%	-	
CFS-2	Cement Fibre sand	6%	1.0%	-	
CGS-1	Cement Geogrid sand	6%	-	Single layer	Type-1 Biaxial Geogrid
CGS-2	Cement Geogrid sand	6%	-	Dual layer	Type-1 Biaxial Geogrid
CGS-3	Cement Geogrid sand	6%	-	Single layer	Type-2 Biaxial Geogrid
CGS-4	Cement Geogrid sand	6%	-	Dual layer	Type-2 Biaxial Geogrid
CFGS-1	Cement Fibre & Geogrid sand	6%	0.5%	Single layer	Type-1 Biaxial Geogrid
CFGS-2	Cement Fibre & Geogrid sand	6%	0.5%	Dual layer	Type-1 Biaxial Geogrid
CFGS-3	Cement Fibre & Geogrid sand	6%	1.0%	Single layer	Type-1 Biaxial Geogrid
CFGS-4	Cement Fibre & Geogrid sand	6%	1.0%	Dual layer	Type-1 Biaxial Geogrid
CFGS-5	Cement Fibre & Geogrid sand	6%	0.5%	Single layer	Type-2 Biaxial Geogrid
CFGS-6	Cement Fibre & Geogrid sand	6%	0.5%	Dual layer	Type-2 Biaxial Geogrid
CFGS-7	Cement Fibre & Geogrid sand	6%	1.0%	Single layer	Type-2 Biaxial Geogrid
CFGS-8	Cement Fibre & Geogrid sand	6%	1.0%	Dual layer	Type-2 Biaxial Geogrid

fibres, the flexural stress increased in proportion to the deflection until the specimen was cracked, and the cracking occurred in a gentler slope condition than the unreinforced specimens. The value then decreased to zero very slowly. This finding illustrated that short fibres increased the first crack strength of the cement-mixed soil and exhibited some deflection before cracking. However, the residual strength (strength after cracking) was not affected. The maximum strength was obtained at the first cracking of beam specimens. The peak flexural strength of unreinforced specimens (CMS-0) was 0.531 MPa, whereas those of the specimens (CFS-1 and CFS-2) reinforced with 0.5% and 1% fibre contents were 0.669 MPa and 0.692 MPa, respectively. These fiber-reinforced specimens exhibited greater deflection than the unreinforced specimens before they reached their peak points and zero stresses. Since the specimen did not experience any bearing capacity recovery stage after cracking due to its short fibre length, its flexural stress deflection behaviour could be classified as deflection softening semiductile behaviour according to ASTM C1609/C1609 M [14].

4.2 Stress–Deflection Curves of Cement Sand Reinforced With Geogrids

The stress–deflection curves of single- and double-geogrid-reinforced cement-mixed sand are shown in Fig 7. The shapes of the deflection curves clearly illustrate that the addition of both types of biaxial geogrids (single and dual layers) affected the flexural characteristics of the cement-mixed sand. For geogrid-reinforced cement-mixed sand, variations in the flexural stress versus deflection response could be divided into five stages: (I) linear elasticity stage, (II) brittle failure stage at the peak stress, (III) bearing capacity recovery stage due to the tensile strength of the geogrid reinforcement, (IV) bearing capacity loss stage, and (V) residual strength stage [11]. The linear elasticity stage was very similar to that of the unreinforced specimens. First, the flexural stress increased in proportion to the deflection until the occurrence of the first crack and the attainment of its first peak strength. The strength then decreased to almost half of the first crack strength. These results indicated that the flexural load transferred to the geogrid right after beam cracking. The weak bond at the geogrid-cement-mixed sand and geogrid interface potentially caused the decline in flexural stress. However, after brittle behaviour and a decrease in strength, the bearing capacity started to recover to a greater level than the first crack strength due to the activation of the tensile strength of the geogrid layers.

During the increase in strength, the deflection graph showed some local brittle behaviour and continuous fluctuations; this behaviour was repeated until the loss of bearing capacity. Compared with the type-1 geogrid-reinforced specimens, specimens reinforced with type-2 geogrid showed a smaller decline in strength after reaching their first peak strength. A greater post-crack flexural stress capacity was observed. This was likely caused by the higher tensile strength of the type-2 geogrid. The repetition of the local declines in the stress–deflection curves that occurred after the first crack (Fig *7*) was a peculiar behaviour which had not been observed in the steel bar reinforced, fibre-reinforced concrete, and cement-mixed soil. It was potentially caused by the weak bonding at the geogrid–cement–mixed sand interface. The weak bond at the geogrid-cement-mixed sand and geogrid interface was more pronounced in the specimens reinforced with type 2 geogrid.

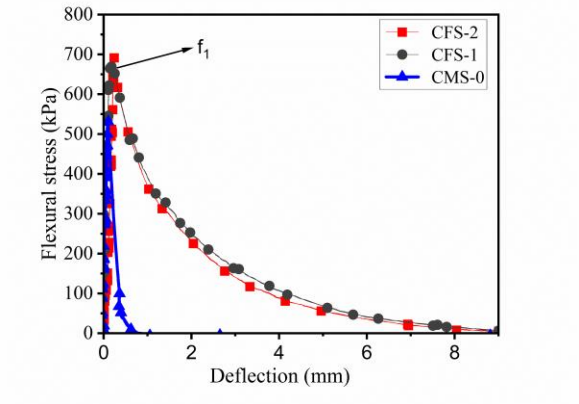

Fig 6. Stress–deflection curves of the unreinforced and fibre-reinforced cement-mixed sand specimens.

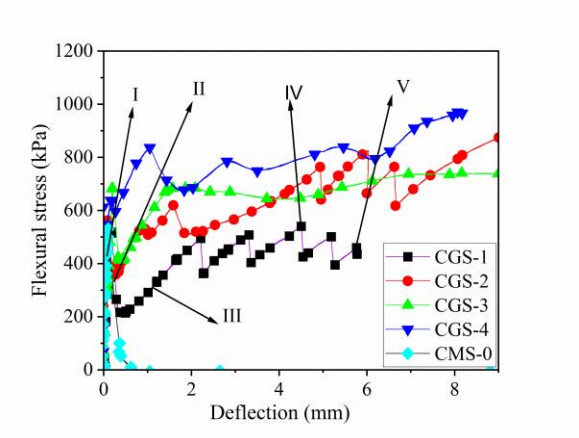

Fig 7. Flexural stress–deflection curves of the cement-mixed sand reinforced with single and dual layers using two different types of geogrids.

4.3 Stress–Deflection Curves of The Specimens Reinforced With Both Fibres And Geogrids

The stress–deflection curves of the specimens reinforced with both fibres and geogrids are shown in Fig 8 and Fig 9. The graph clearly illustrates that the addition of both short fibres and geogrid layers significantly affected the stress–deflection curve. When the sample was reinforced with a single layer of geogrid and 0.5% or 1% fibre, the flexural stress proportionally increased with increasing deflection from zero to the occurrence of the first crack in the bottom of the beam. However, the decline in strength after the specimen cracked was not significant. The bearing capacity of specimens reinforced with both fibres and geogrids recovered immediately after a negligible drop occurred after the first cracking. These results indicate that the addition of fibres improved the local brittle behaviour that was observed in samples reinforced with only geogrids (Fig 7). Moreover, fluctuations in the deflection curves of the geogrid cement sand specimens were not observed due to the influence of the fibre addition. When the beam initially cracks, the geogrid could not bear all the applied load since the geogrid was still at low strain. When cracks propagated, a loss in strength occurred. However, in these specimens, the fibres started bearing the loads before beam cracking, as was observed in the fibre-reinforced samples; thus, the first crack strength of the specimens increased. In addition, the samples reinforced with dual geogrid layers and 1% fibre exhibited more deflection before reaching the first crack. Moreover, no significant drop was observed in the deflection curve after the first cracking of the beam. These showed that fibres could avoid the sudden loss of flexural strength immediately after the first cracking occurred. Finally, the stress–deflection curves of the specimens reinforced with the dual geogrid layer and the 1% fibre mixture were very similar to those of the steel-reinforced concrete [16, 17]. Compared to those of the other reinforcement types, the stress–deflection curve characteristics of these samples exhibited the greatest improvement. Compared to those reinforced with type-1 geogrids, samples reinforced with type-2 geogrids exhibited a smaller decline in strength right after the occurrence of the first crack. Additionally, the strength of the samples reinforced with type-2 geogrids was relatively greater than those reinforced with type-1 geogrids because of the higher tensile strength of the type-2 geogrids.

4.4 Crack Pattern and Failure Mode

Crack patterns, such as the shape and failure mode of the cement-mixed beams, were observed during the test. Crack patterns can be used as one of the main parameters for characterizing the performance of treated soil [4, 11]. Four types of crack patterns were observed in all specimens. The first type of crack (Fig 9 a, and b) was a common single tensile crack that occurred at the mid-span of the beam and then propagated to the top of the beam. Although the CFS-1 and CFS-2 specimens had greater flexural strength than the CMS-0 specimens, the reinforcement was not able to recover the load-bearing capacity after the occurrence of the first crack in the specimen. The second type of crack was also a single crack (Fig 10c,

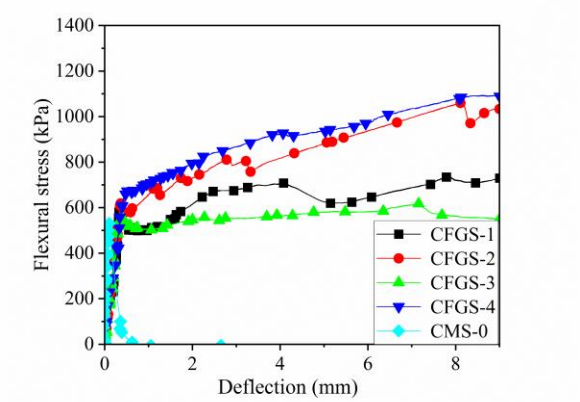

Fig 8 .Stress–deflection curves of the samples reinforced with both fibres and type-1 geogrids

and d), followed by a horizontal crack at the position of the geogrid layer at the bottom of the beam. The horizontal crack propagated with deflection, followed by the breaking off of the bottom cover of the beam, which started at the mid-span and propagated to the beam supports. These cracks were observed in both; the cement-mixed geogrid sand, and the cement-mixed sand specimens reinforced with a single geogrid layer. The cracks revealed that the geogrid did not start bearing stress at the initial stage before cracking due to the weak bond between the cement mix and the geogrid. The third type of crack (Fig 10e) was a combination of vertical tensile cracks: diagonal shear cracks and horizontal cracks. These cracks were observed in the sample reinforced with 0.5% fibre and the dual geogrid layers. This finding showed that the fibre material could increase flexural strength and avoid horizontal cracks and geogrid cover separation. However, the fibre content was not sufficient to prevent it completely. The sample failed with propagation of the shear crack in the fourth type of crack (Fig 10f), small tensile cracks started at the bottom midspan and increased towards the supports,

and propagated to the top of the beam. The sample failed with the propagation of cracks to the support and top. These behaviours were observed in samples reinforced with 1% fibre and two layers of geogrid, were quite similar to those of a reinforced concrete beam [16, 17] and resulted in the highest flexural strength and flexural performance.

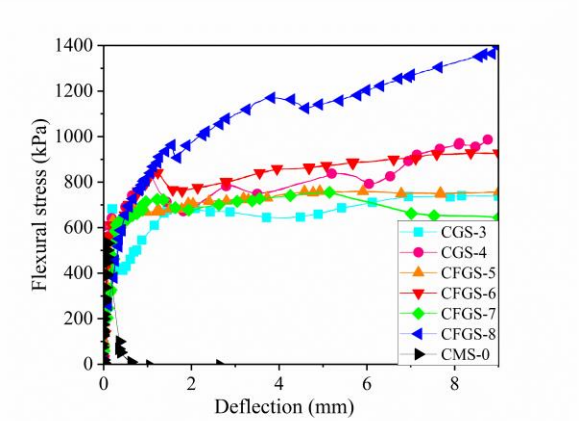

Fig 9. Stress–deflection curves of the samples reinforced with both fibres and type-2 geogrids.

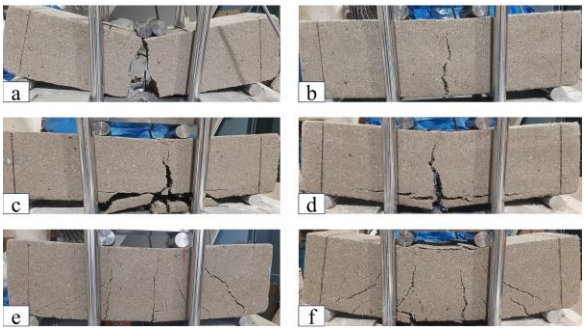

Fig 10. Crack patterns: (a) CMS-0; (b) CFS-2; (c) CGS-1; (d) CFGS-3; (e) CGS-2; (f) CFGS-2

5. CONCLUSIONS

In this study, the effects of a biaxial geogrid and short PVA fibre content on cement-mixed sandy soil were investigated. The parameters such as the flexural stress deflection curve, crack pattern, and failure mode were studied. On the basis of the experimental results, the following conclusions can be drawn:

1. The characteristics of the stress–deflection curve of the cement–mixed sand were affected by the addition of fibres and geogrids. The fibre addition (0.5% and 1%) increased the first peak flexural strength (strength before cracking of the beam at its bottom face) by 1.26 and 1.3, respectively, and resulted in semi-ductile behaviour. However, the effect on the overall flexural strength was insignificant due to its short length. Adding a single geogrid layer and dual geogrid layer improved the peak flexural strength by 1.3 to 1.87, and resulted in more deformation before failure.
2. The strength of the cement-mixed sand reinforced with a single geogrid layer and dual geogrid layer significantly decreased immediately after the occurrence of the first crack and recovered very late; this effect was not observed in the samples reinforced with both short-fibre cement-mixed sand and geogrids, which experienced greater deflection.
3. The stress–deflection curves of the cement-mixed specimens reinforced with 1% fibre and a dual layer of geogrid were very similar to the stress–deflection curves of the steel bar–reinforced concrete. This geogrid reinforcement distributed the stresses from a single crack plane to the different parts of the beam and exhibited a multiple-plane failure mode.
4. The cement-mixed specimens reinforced with 1% fibre and a dual geogrid layer had the highest flexural strength (first peak, peak, and residual), lowest brittleness index, greatest improvement in the stress–deflection curve, and greatest improvement in the failure mode among the other samples. Based on these findings, geogrid reinforcement and fibres are suitable reinforcement for cement-mixed soils used in base and subbase coarse applications.

6. ACKNOWLEDGEMENT

The authors would like to acknowledge the Geosphere and Geotechnical Laboratory of the Department of Civil and Environmental Engineering, Saitama University, for providing equipment and materials for this research.

7. REFERENCES

[1] Sukontasukkul P., & Jamsawang P., Use of steel fibre improve flexural performance of deep soil–cement column. Construction and Building Materials, Vol. 29, Issue 2012, pp. 201-205.

[2] Disfani M. M., Arulrajah A., Haghihi H., Mohammadinia A., and Horpibulsuk S., “Flexural beam fatigue strength evaluation of crushed brick as a supplementary material in cement stabilized recycled concrete aggregates.” Construction and Building Materials, 68, Issue 3, 2014, pp. 667–676.

[3] Jamsawang P., Voottipruex P., & Horpibulsuk S., Flexural strength characteristics of compacted cement-polypropylene fiber sand. Journal of

Materials in Civil Engineering, Vol. 27, 2014, pp. 04014243.

[4] Chindaprasirt P., Jamsawang P., Sukontasukkul P., Jongpradist P., & Likitlersuang S., Comparative mechanical performances of cement-treated sand reinforced with fiber for road and pavement applications. Transportation Geotechnics, Vol. 30, 2021, pp. 100626.

[5] Suleman M., Ahmad N., Khan S. U., & Ahmad T., Investigating flexural performance of waste tires steel fibers-reinforced cement-treated mixtures for sustainable composite pavements. Construction and Building Materials, Vol. 275, 2021, pp. 122099.

[6] Yao X., Huang G., Wang M., & Dong X., Mechanical properties and microstructure of PVA fiber reinforced cemented soil. KSCE Journal of Civil Engineering, Vol. 25, 2021, pp. 482-491.

[7] Shen Y. S., Tang Y., Yin J., Li M. P., & Wen T., An experimental investigation on strength characteristics of fiber-reinforced clayey soil treated with lime or cement. Construction and Building Materials, Vol. 294, 2021, pp. 123537.

[8] Ateş A., Mechanical properties of sandy soils reinforced with cement and randomly distributed glass fibers (GRC). Composites Part B: Engineering, Vol. 96, 2016, pp. 295-304.

[9] Sukontasukkul P., & Jamsawang P., Use of steel and polypropylene fibers to improve flexural performance of deep soil–cement column. Construction and Building Materials, Vol. 29, 2012, pp. 201-205.

[10] Park S. S., Effect of fiber reinforcement and distribution on unconfined compressive strength of fiber-reinforced cemented sand. Geotextiles and Geomembranes, Vol. 27, Issue 2, 2009, pp. 162-166.

[11] Chuenjaidee S., Jamsawang P., Jongpradist P., & Chen X., Flexural Performance of Cement-Treated Sand Reinforced with Geogrids for Use as Sub-Bases of Pavement and Railway Structures. Materials, Vol. 15, 2022, pp. 2877.

[12] Suparma, L. B., & Rifa'i, A., Determination Of Optimum Cement Content For Silty Sand Soil Stabilization As The Base Course. International Journal of GEOMATE, Vol. 26, Issue 115, March 2024, pp. 124-133.

[13] ASTM C1609/C1609 M; Standard Test Method for Flexural Performance of Fiber-Reinforced Concrete. ASTM International, 2019, pp. 1-9.

[14] Tatsuya Nukushina, Kenzo Watanabe, Saeka Fujioka, Kazuya Murata, Goro Sakai and Noboru Sakata (2015). New Sheet Curing Method for Enhancing Durability of Concrete, Annual report, Kajima Technical Research Institute, Kajima Corporation, Vol. 63, 2015, pp. 103-108.

[15] Kim Y. T., & Kang H. S., Engineering characteristics of rubber-added lightweight soil as a flowable backfill material. Journal of Materials in Civil Engineering, Vol. 23, Issue 9, 2011, pp. 1289-1294.

[16] Arezoumandi M., Smith A., Volz J. S., & Khayat K. H., An experimental study on flexural strength of reinforced concrete beams with 100% recycled concrete aggregate. Engineering Structures, Vol. 88, 2015, pp. 154-162.

[17] Cuong T. V., Tan N. N., Kawamoto K., & Giang N. H., Flexural Behavior of Reinforced Concrete Beams Using Synthetic Aggregates Produced From Waste Powder in VietnamInternational Journal of GEOMATE, Vol. 27, Issue 120, Aug, 2024, pp. 69-76.